Visualizing dynamic cytoplasmic forces with a compliance-matched FRET sensor

Fanjie Meng and Frederick Sachs*

Center for Single Molecule Biophysics, Department of Physiology and Biophysics, State University of New York at Buffalo, 3435 Main Street, Buffalo, NY 14214, USA

*Author for correspondence (sachs@buffalo.edu)

Accepted 27 September 2010
Journal of Cell Science 124, 261-269

doi:10.1242/jcs.071928

Summary

Mechanical forces are ubiquitous modulators of cell activity but little is known about the mechanical stresses in the cell. Genetically encoded FRET-based force sensors now allow the measurement of local stress in specific host proteins in vivo in real time. For a minimally invasive probe, we designed one with a mechanical compliance matching that of many common cytoskeleton proteins. sstFRET is a cassette composed of Venus and Cerulean linked by a spectrin repeat. The stress sensitivity of the probe was measured in solution using DNA springs to push the donor and acceptor apart with 5–7 pN and this produced large changes in FRET. To measure cytoskeletal stress in vivo we inserted sstFRET into α-actinin and expressed it in HEK and BAEC cells. Time-lapse imaging showed the presence of stress gradients in time and space, often uncorrelated with obvious changes in cell shape. The gradients could be rapidly relaxed by thrombin-induced cell contraction associated with inhibition of myosin II. The tension in actinin fluctuated rapidly (scale of seconds) illustrating a cytoskeleton in dynamic equilibrium. Stress in the cytoskeleton can be driven by macroscopic stresses applied to the cell. Using sstFRET as a tool to measure internal stress, we tested the prediction that osmotic pressure increases cytoskeletal stress. As predicted, hypotonic swelling increased the tension in actinin, confirming the model derived from AFM. Anisotonic stress also produced a novel transient (~2 minutes) decrease in stress upon exposure to a hypotonic challenge, matched by a transient increase with hypertonic stress. This suggests that, at rest, the stress axis of actinin is not parallel to the stress axis of actin and that swelling can reorient actinin to lie more parallel where it can absorb a larger fraction of the total stress. Protein stress sensors are opening new perspectives in cell biology.

Key words: Actinin, Fluorescence energy transfer, Force, FRET, Osmotic pressure, Sensor, Stress

Introduction

Cells have three primary sources of energy: chemical potential, electrical potential and mechanical potential and only the first two are well studied. Mechanical stress is a universal variable that affects multiple physiological and pathological processes, including angiogenesis, osteogenesis, osteoporosis, muscle growth, muscular dystrophy, aortic aneurysms and tumor growth (Kumar and Weaver, 2009; Wallace and McNally, 2009) as well as embryonic development, including differentiation and apoptosis (Shyu, 2009; Vogel and Sheetz, 2006). The dissipation of stress from local sites of stimulation and the transduction of stress into biochemical signals takes place at multiple length scales that range from biomolecules to ballerinas and on a variety of time scales from milliseconds (Bustamante et al., 2004; Kung, 2005; Na et al., 2008) to years. To understand the role of mechanical forces in cell biology, we need to be able to measure the stress distribution in specific proteins in vitro, in vivo and in situ because the cytoskeleton is inhomogeneous and anisotropic. Several years ago we developed a Förster resonance energy transfer (FRET)-based force cassette that utilized two GFPs (Venus and Cerulean) linked with an α-helix that could be inserted into a variety of proteins (Fanjie Meng; stFRET, a novel tool to study molecular force in living cells and animals, PhD thesis, State University of New York at Buffalo, 2008); Meng et al., 2008). Iwai and Uyeda later used a similar approach to investigate ligand-induced stress in myosin (Iwai and Uyeda, 2008).

The sensitivity of a fluorescent stress sensor is limited by the shot noise of the fluorophores and the thermal fluctuations of stress in the host and the probe. If the force–distance relationship of the linker is nonlinear, as occurs in subunit unfolding, the force sensitivity can be increased at the expense of linearity. An ideal probe would also have the same mechanical compliance as its host protein so that it would cause minimal interference with the normal physiological function of the host. With these goals in mind, we constructed a force probe that uses a spectrin repeat as the linker. Termed ‘sstFRET’ (spectrin stFRET) we measured its force sensitivity in solution using DNA springs (Zocchi, 2009). These are floppy loops of single-stranded DNA (ssDNA) covalently bound to two distant sites in the probe. Because it is floppy, ssDNA does not cause much stress in the protein. However, when complementary DNA is added, the double-stranded DNA (dsDNA) has a much longer persistence length, which causes the loop to straighten and push apart the fluorophores with 5–7 pN (Qu et al., 2010) and thus decreases FRET.

To examine in vivo stresses, we transfected HEK and BAEC cells with actinin-sstFRET and used time-lapse imaging to measure the stress distribution in time and space. We found that cells spontaneously undergo large changes in stress that were often not correlated with changes in cell shape, and thus were previously undetected. Stimulating the cells with thrombin, which inhibits myosin II, rapidly induces a variety of inflammatory responses (Bogatcheva et al., 2002; Garcia, 1992) that make the cells rapidly contract. This contraction was associated with decreased stress in actinin, suggesting that actinin is mechanically not in series with actin.

Journal of Cell Science

Using sstFRET we tested the hypothesis that osmotic stress in cells is not confined to the membrane but is shared by the cytoskeleton (Spagnoli et al., 2008). We applied anisotonic stress to HEK and BAEC cells transfected with sstFRET-actinin. The stress increased with swelling as predicted by atomic force microscopy (AFM) (Spagnoli et al., 2008), graphically illustrating that osmotic stress is distributed in three dimensions and not confined to the two dimensions of the membrane. We also observed a novel transient (~2 minute) decrease in stress (increase of FRET) with hypotonic challenge, and an inverse increase in stress with a hypertonic challenge. This suggests that the actinin axis at rest is not parallel to the force generating the actin filament axis, but that the actinin axis becomes more parallel as the stress increases.

Results

Development and characterization of sstFRET

Fig. 1A shows the basic structure of the sstFRET cassette. The linker was subcloned from non-erythrocytic (α-fodrin) isoform 1 (NCBI reference sequence: NP_001123910), using the sequence from amino acid phenylalanine 1238 to lysine 1334. We added two glycines flanking each end of the repeat to provide flexibility. We then characterized the physical properties of purified sstFRET protein by modifying the linker (An et al., 2006; Ortiz et al., 2005) with urea, trypsin and temperature (supplementary material Fig. S1A–C). The fluorophores are remarkably resistant to all three perturbations (Fanjie Meng; stFRET, a novel tool to study molecular force in living cells and animals, PhD thesis, State University of New York at Buffalo, 2008); Meng et al., 2008). The linker unfolded upon treatment with 1–8 M urea, decreasing FRET as the probes moved apart. Cleavage of the linker with trypsin eliminated FRET (supplementary material Fig. S1D,E), but surprisingly, elevated temperature reversibly increased FRET efficiency. This increase could be caused by increased thermal energy acting to bend the linker and thus bring the fluorophores closer together.

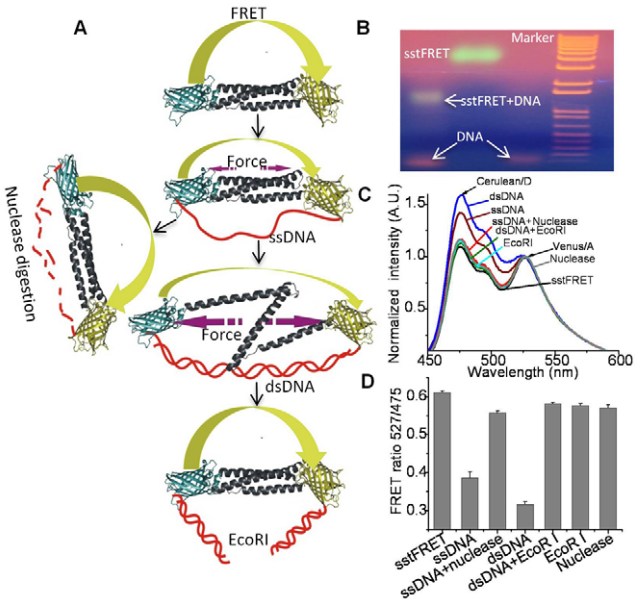

Fig. 1. sstFRET and in vitro DNA stretching. (**A**) Scheme of sstFRET structure and the DNA stretching experiments. Cyan represents the donor Cerulean and yellow the acceptor Venus. The black coiled-coil part represents the spectrin repeat domain and the red lines denote DNA. Purple arrows show the direction of force and the width of the arrows indicates the force. Yellow arrows show energy transfer of sstFRET and the arrow width indicates efficiency. (**B**) sstFRET–DNA complex on an agarose gel. First lane (right): the yellow upper band is the bound complex and the red lower band is unbound DNA. The green band in the second lane is sstFRET, and the third lane is free DNA (red). (**C**) Spectra of the complex before and after various treatments. Excitation at 433 nm and emission scan at 450–600 nm. The spectra intensities were normalized to the Venus acceptor emission peaks to emphasize the changes in acceptor emission. (**D**) Calculated FRET ratio of sstFRET–DNA complexes. One-tailed *t*-tests show that the sstFRET+ssDNA FRET ratio is significantly greater than sstFRET+dsDNA ratio ($P<0.01$). Values are means + s.e.m. ($n=3$). Enzyme treatments with nuclease and *Eco*RI did not affect the FRET ratio of the protein cassette (C,D).

To investigate the force sensitivity of sstFRET, we pushed the fluorophores apart using DNA springs (Zocchi, 2009) linked to the external cysteines in each GFP. The contour length of a 60mer of ssDNA is ~20 nm and the persistence length is about 1 nm. Because the end-to-end distance of sstFRET is ~12 nm, the ssDNA loop is floppy. Adding a complementary strand of DNA creates dsDNA with a persistence length of ~50 nm, pushing apart the two fluorophores with ~20 kT of free energy (k being the Boltzmann constant and T temperature) (Tseng et al., 2009), comparable to the difference in energy between the folded and unfolded configurations of a 100 amino acid protein (Zocchi, 2009). Zocchi's group has shown that the stress produced by dsDNA in this configuration is 5–7 pN, limited in magnitude by kinks that develops in highly curved dsDNA (Qu et al., 2010). The most complaint part of sstFRET is the spectrin repeat that will rapidly unfold at ~20 pN (Law et al., 2003). The GFP fluorophores are rigid and capable of withstanding 100 pN without unfolding (Dietz and Rief, 2004).

To drive the probe with the DNA springs, we first made sstFRET protein by fusing the sstFRET gene to vector pET-52b (+) (Novagen). We then purified the protein and covalently attached a 60mer of thiolated ssDNA (cf. Fig. 1A) (Hwang et al., 2009). The reaction of thiolated DNA to the protein was readily visualized by electrophoresis (Fig. 1B). Under UV light, sstFRET fluoresces green and DNA stained with ethidium bromide fluoresces red, but when sstFRET is bound to DNA, the complex fluoresces yellow. Due to the negative charges of DNA added to the protein, the complex (Fig. 1B, yellow band) migrates faster than the free protein (Fig. 1B, green band). We studied plain sstFRET and sstFRET bound to DNA in solution.

Donor (Cerulean) excitation was at 433 nm and the emission was scanned from 450 nm to 600 nm. Fig. 1C shows the spectra with the amplitudes normalized to the Venus emission peak. Adding the ssDNA loop slightly reduced the FRET ratio relative to unliganded sstFRET (0.40–0.6, respectively) (Fig. 1D). The ssDNA might have pushed the fluorophores apart by a small amount or changed their relative angles. Whatever the cause, this energy could be released by cleavage of ssDNA with nucleases (Fig. 1A,C,D). Adding the complementary strand of DNA pushed the fluorophores apart, decreasing the FRET ratio to ~0.3. The stress from dsDNA could be relieved by cleavage with *Eco*RI because the cut site is in the middle of the loop. Thus, sstFRET is sensitive to forces in the physiologically relevant range and presents a wide dynamic range so that 5–7 pN can cause a 50% decrease in FRET.

Measurements in living cells

Actinin is a cytoskeletal crosslinker that forms homodimers between parallel actin filaments, where it functions as support scaffolding (Sjoblom et al., 2008). As a member of the spectrin superfamily,

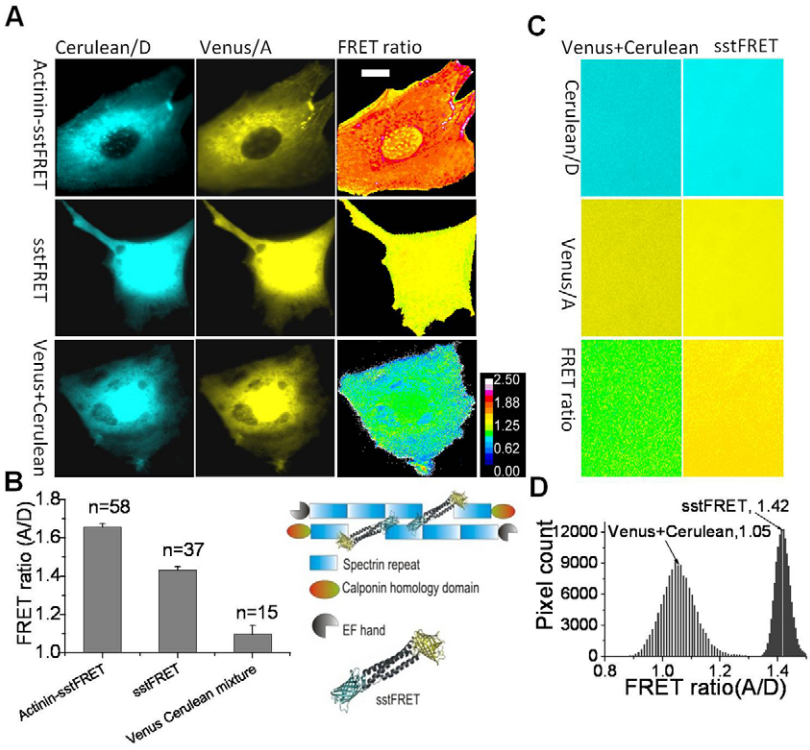

Fig. 2. FRET measurements of sstFRET in living cells and in solution. (**A**) Images of cells expressing actinin-sstFRET, sstFRET alone and Venus+Cerulean 1:1. Cerulean/donor intensity is shown in cyan and Venus/acceptor intensity in yellow; calibration bar of a 16 color lookup table is given on the right. The cartoon inset shows the homologous domains of actinin and the relative position of the sstFRET cassette. (**B**) Comparison of the FRET ratio of the three cell groups. The baseline was set at 1.0 and the ratio observed with no energy transfer. (**C**) Solution images measuring donor, acceptor and FRET ratio images of sstFRET protein, and a 1:1 mixture of donor and acceptor fluorophores in solution. (**D**) Histograms of pixel counts showing no saturation of any channel. A one-tailed *t*-test shows that FRET of the actinin-sstFRET group is greater than that of the free sstFRET group, and that the sstFRET group is greater than that of the Venus+Cerulean coexpressing group ($P<0.01$). Scale bar: 10 µm. The lookup table is 16 colors.

actinin is made of four spectrin repeat domains, an actin binding domain and a calmodulin homology domain (Golji et al., 2009). sstFRET with its spectrin repeat linker should be able to monitor stress in actinin with minimal perturbation of the host, and we genetically incorporated sstFRET between spectrin repeat domains 1 and 2 in α-actinin (Fig. 2, cartoon inset). Transfecting BAEC and HEK cells with plasmids encoding actinin-sstFRET produced fluorescent cells that were sensitive to mechanical stress. As controls, we expressed both the stress-free plain cassette and a 1:1 mixture of Venus and Cerulean.

To calculate the FRET efficiency we explored methods that were reliable, independent of concentration and insensitive to the differential bleaching rates of the donor and acceptor (cf. supplementary material Figs S2–S4). We found that the best method was to measure the donor signal with donor excitation and the acceptor signal with acceptor excitation. This avoided the need for additional bleed-through corrections (see Materials and Methods). After subtracting background, we divided the acceptor image by the donor to obtain the FRET ratio. From the ratio we calculated the FRET efficiency of the unstressed probe to be ≈26% in both solution and in cells.

As expected for a crosslinked donor and acceptor, cells expressing plain sstFRET showed a significantly higher FRET ratio than cells expressing a 1:1 mixture of the individual donors and acceptors (Fig. 2A,B). Surprisingly, resting cells expressing actinin-sstFRET showed higher FRET ratio (the fluorophores were closer or better aligned) than cells expressing the sstFRET cassette alone. This might be caused by actinin homodimerization compressing sstFRET or altering the fluorophore angles (see also supplementary material Fig. S1C). We ruled out intermolecular energy transfer between different actinin dimers because the FRET ratio was independent of expression level (supplementary material Figs S2, S3). Energy transfer between antiparallel actinins within a dimer was also unlikely because the fluorophores are too far apart. Unstressed free sstFRET in cells had a FRET ratio of 1.42, similar to that of the protein in solution. A 1:1 mixture of free donors and acceptors in cells gave a FRET ratio (1.05) that was the same as the mix of the two fluorophores in solution (Fig. 2C,D).

Actinin-sstFRET localization in BAEC and HEK cells

To examine whether inserting a relatively large probe like sstFRET into actinin affects the cell biology, we compared the distribution to chimeric terminally labeled actinin-EGFP (a more traditional label) (Fig. 3). The actinin distribution of both labels in HEK cells were indistinguishable, showing smooth actin fiber networks tagged by actinin (Fig. 3A). In BAECs, both actinins displayed a periodic localization along actin fibers (Fig. 3B). Cells de-membranated with Triton X-100 retained the actinin localization seen in the living cell. The distinct localization patterns of actinin between HEKs and BAECs imply divergent roles for actinin stemming from the time of differentiation.

Colocalization of actinin-sstFRET with actin stress fibers and focal adhesions

To further test that labeled actinin did not interfere with normal physiological function, we examined how actinin colocalized to both focal adhesions and actin fibers (Fig. 4) using fixed cells. We expressed free sstFRET (a control), actinin-EGFP and actinin-sstFRET in BAECs and then fixed and stained the cells with phalloidin–Alexa Fluor 568. Both actinin-sstFRET and actinin-EGFP displayed the same periodic distribution along actin (Fig. 4A). Because actinin scaffolds actin at focal adhesions, and vinculin is well known to bind to focal adhesions (Coll et al., 1995), we also used anti-vinculin antibodies with a secondary antibody conjugated to Alexa Fluor 633 to colabel focal adhesions

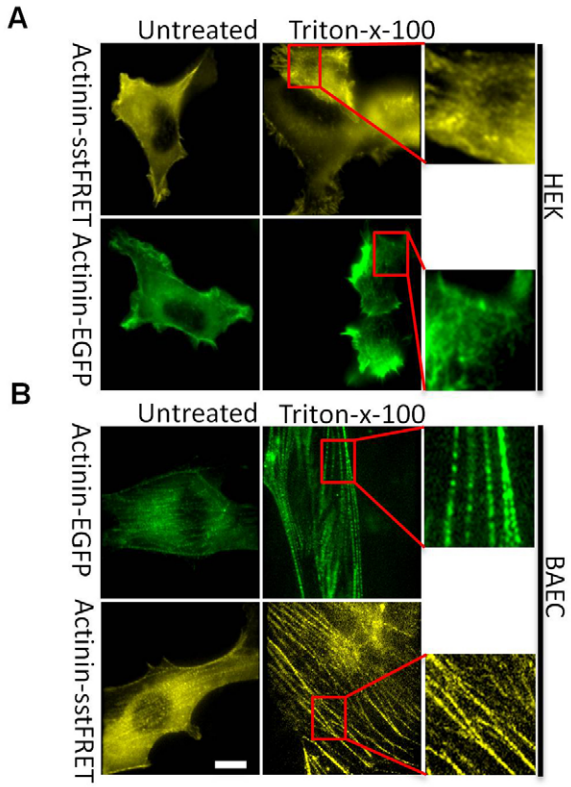

Fig. 3. Protein distribution of actinin-sstFRET and actinin C-terminal–EGFP. Studies were carried out using (**A**) HEK and (**B**) BAEC cells with and without Triton X-100 treatment to remove membranes. Actinin-sstFRET distributions are displayed as the Venus/acceptor images and the actinin–EGFP distributions as EGFP images. The distribution of labeled actinin is similar with both probes. Enlarged images of the boxed areas are shown on the right. Scale bar: 10 μm.

(Fig. 4B). Vinculin colocalized with both actinins but not with free sstFRET, confirming that actinin-sstFRET is an innocuous probe of actinin stress.

Cytoskeletal stresses in living cells

Contraction, migration and mitosis are accompanied by biochemical changes that are likely to be accompanied by mechanical changes. We recorded 1000 minutes of time-lapse images of labeled HEK cells in normal media at room temperature (see Materials and Methods) (Fig. 5A,B). Looking at the cells in Fig. 5, the FRET ratio increased slightly during the first 100 minutes (to frame 5), then decreased until 800 minutes (frame 40), and then increased again during the next 200 minutes. A video clip of the time series shows the correlation between stress and structural remodeling (see supplementary material Movies 1 and 2). We found a wide variety of stress modulation profiles, even between adjacent cells in the same dish (Fig. 5C). For example (Fig. 5), Cell 1 showed a gradual decline increase of stress. Cell 5 showed a relaxation of stress and then a plateau that remained stable to the end of the time series. Cells 2, 3 and 4 displayed more complex patterns in time and space (Fig. 5C). These widely variable gradients emphasize the heterogeneity of clonal cells. We observed no time-dependent changes in FRET for cells expressing the free probe, which argues that the stresses we observed arose from mechanical coupling through actinin (Fig. 5D,E). The sstFRET signals not only displayed the slow gradients of the time-lapse series but also high frequency (seconds) fluctuations demonstrating that the stress in actinin is dynamic. There were no such fluctuations in cells expressing the free cassette.

Thrombin induces rapid changes in actinin stress

Thrombin causes endothelial cell contraction by inactivating myosin light chain phosphatase (Essler et al., 1998) and we studied how these changes affect the stress in actinin. We observed the cited contractions in cells expressing actinin-sstFRET (Fig. 6A). Thrombin produced an immediate decrease of tension followed by a sustained increase. The increase appears to represent a relaxation of constitutive stress by contraction of parallel myosin (Fig. 6A, FRET ratio plotting panels). Thrombin also reduced the magnitude of force fluctuations compared to the control cells (Fig. 6B) consistent with an inhibition of myosin activity. Cells expressing free sstFRET also contracted with thrombin, but they exhibited no change in FRET (Fig. 6C). These results support use of our FRET calculation methodology ratio because there were large changes in cell anatomy but no change in FRET for the free probe.

Migrating cells

Migrating cells generate forces on the substrate that are larger at the leading edge than at the trailing edge (du Roure et al., 2005). These forces must be matched by internal stresses in the cytoskeleton, and we found that actinin had higher stress at the leading edge and lower stress at the trailing edge (Fig. 6A,D, FRET ratio image). As mentioned above, actinin in these cells showed large amplitude and high speed force fluctuations (compare Fig. 6D and 6E).

Force loading on actinin during an osmotic challenge

AFM experiments suggest that osmotic stress is not confined to the cell membrane but is supported mostly by the cytoskeleton (Spagnoli et al., 2008). We tested the prediction by measuring actinin stress in cells subjected to anisotonic solutions. Initially we challenged HEK cells (Fig. 7) and BAEC cells (Fig. 8) with distilled water to exaggerate any effects. Some HEK cells quickly lysed (although BAECs could withstand distilled water for more than an hour). To allow for more stable measurements with HEK cells, we titrated them with 30%, 50%, 75% and 85% distilled water (in saline) (Fig. 7A). For the first 2 minutes in 30% distilled water, we observed a transient increase in FRET, implying a decrease in tension. Although we thought this might be an effect of decreasing local ionic strength as water entered the cell, we varied ionic strength on sstFRET in solution and found no effect. The paradoxical transient response to a hypotonic shock has not been previously reported. As discussed below, the effect might represent a reorientation of actinin relative to the axis of actin tension. After the transient response, the cells began to swell (as expected) and actinin stress increased.

We then switched to 50% distilled water for 20 minutes and then 75% distilled water, and found that the FRET ratio continued to decline. After 10 minutes of 75% distilled water, the FRET ratio had decreased by more than 20% (from 1.8 to 1.4; Fig. 7B,C). When cells were returned to bath saline, they shrank and the stress relaxed. We then performed another round of challenges using 75% and 85% distilled water. The FRET ratio showed a larger decline (31%, from a ratio of 1.6 to 1.1) compared with the original challenge (1.1 was the FRET ratio observed in cells co-transfected with a 1:1 mixture of Venus and Cerulean; cf. Fig. 2). The low FRET ratio could be the

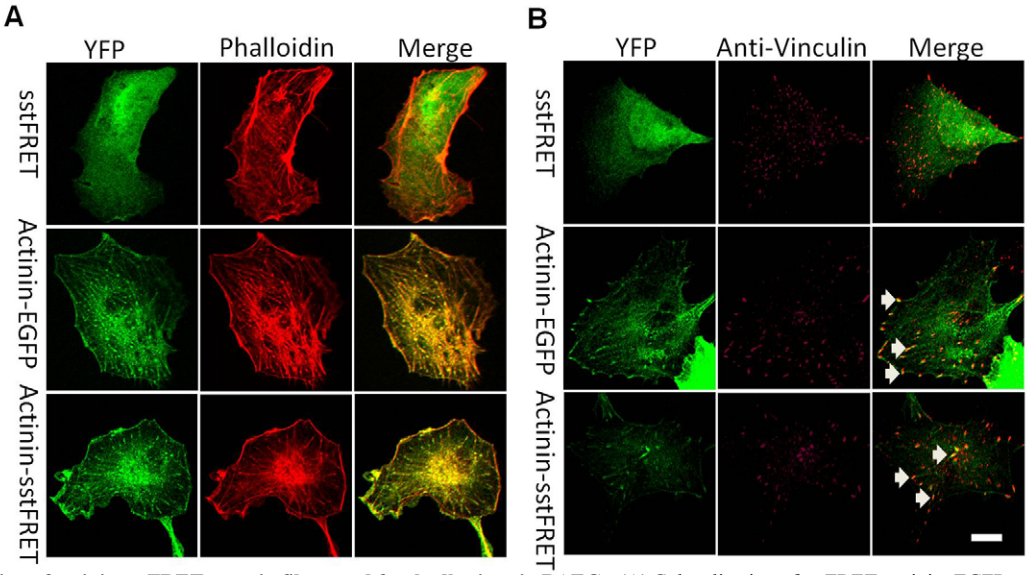

Fig. 4. Colocalization of actinin-sstFRET to actin fibers and focal adhesions in BAECs. (**A**) Colocalization of sstFRET, actinin–EGFP and actinin-sstFRET with actin stained with phalloidin–Alexa Fluor 568. YFP panels show signals from the acceptor Venus in sstFRET and actinin-sstFRET, and signals from EGFP in actinin–EGFP indicating the localization of these chimeric proteins. Phalloidin panels show actin fibers. (**B**) Colocalization of sstFRET, actinin–EGFP and actinin-sstFRET with vinculin immunostained by anti-vinculin and Alexa-Fluor-633-conjugated goat anti-rabbit secondary antibodies. Arrows point to the focal adhesions. Scale bar: 10 µm.

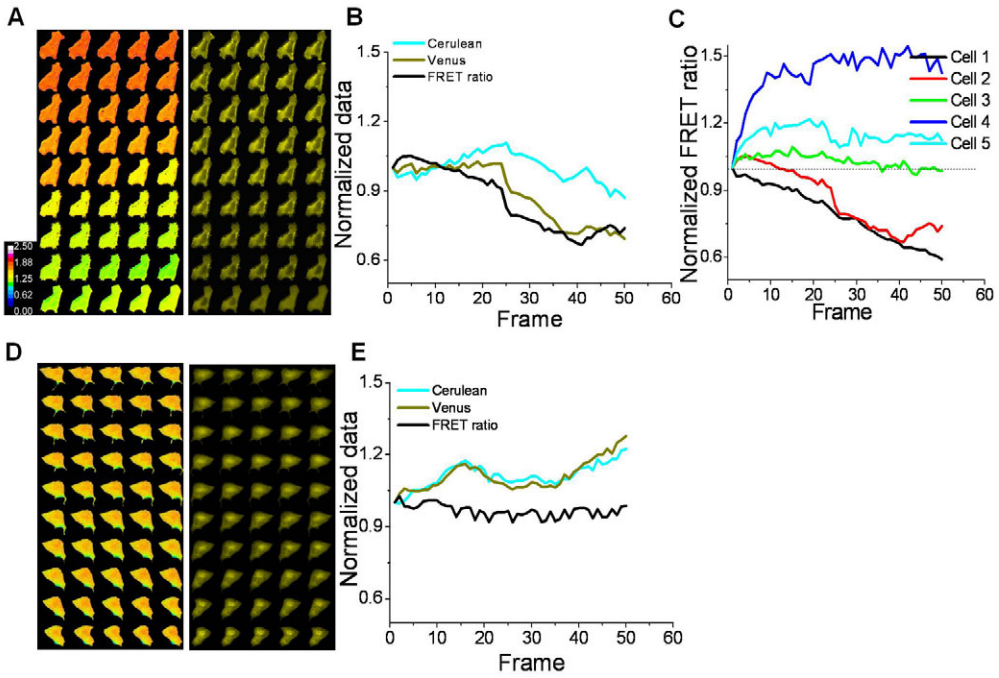

Fig. 5. Stress modulation in actinin in resting HEK cells. (**A**) Montage of FRET ratio images (left panel, 16 color lookup table with a calibration bar from 0 to 2.5) and Venus/acceptor images (right panel) from a 1000-minute time series (50 frames at 20-minute intervals). Venus and Cerulean image intensities were assigned to yellow and cyan, respectively. (**B**) Plot of the normalized average value of Venus/acceptor intensity, Cerulean/donor intensity and FRET ratios from each frame showing continuous stress changing in actinin. All data were normalized to the value of the first frame. In the first 25 frames, the sstFRET protein level was constant (green trace), the FRET ratio decreased (black trace), the Cerulean signal (cyan trace) increased due to the corresponding decrease in FRET. From frames 25 to 50, protein concentration gradually decreased and the FRET ratio also decreased until frame 40 and then started to increase. (**C**) The FRET ratios from five different cells over a 1000-minute time series. The cells displayed distinct time dependencies of the stress: cell 1, increasing stress; cell 2, decreasing stress during the first 5 time frames then increasing until time frame 40, then decreasing again; cell 3, the stress remained constant (also showing that bleaching was not a problem); cell 4, the stress decreased then flattened at frame 30; cell 5, the stress decreased then increased at frame 22, then flattened until frame 50. (**D**) Cells expressing free sstFRET as control for stress modulation in actinin. Montage of FRET ratios (left panel) and Venus/acceptor intensities (right panel) from a 1000-minute time series of an HEK cell expressing free sstFRET. Images show that stress-free sstFRET cannot sense any stress changing in cytoskeleton, ruling out any artificial effects in A. (**E**) Plot of the normalized average value of Venus/acceptor intensity, Cerulean/donor intensity, and FRET ratios from each frame in D, showing the flat FRET ratio through the entire time series despite the fluctuations of donor and acceptor intensity.

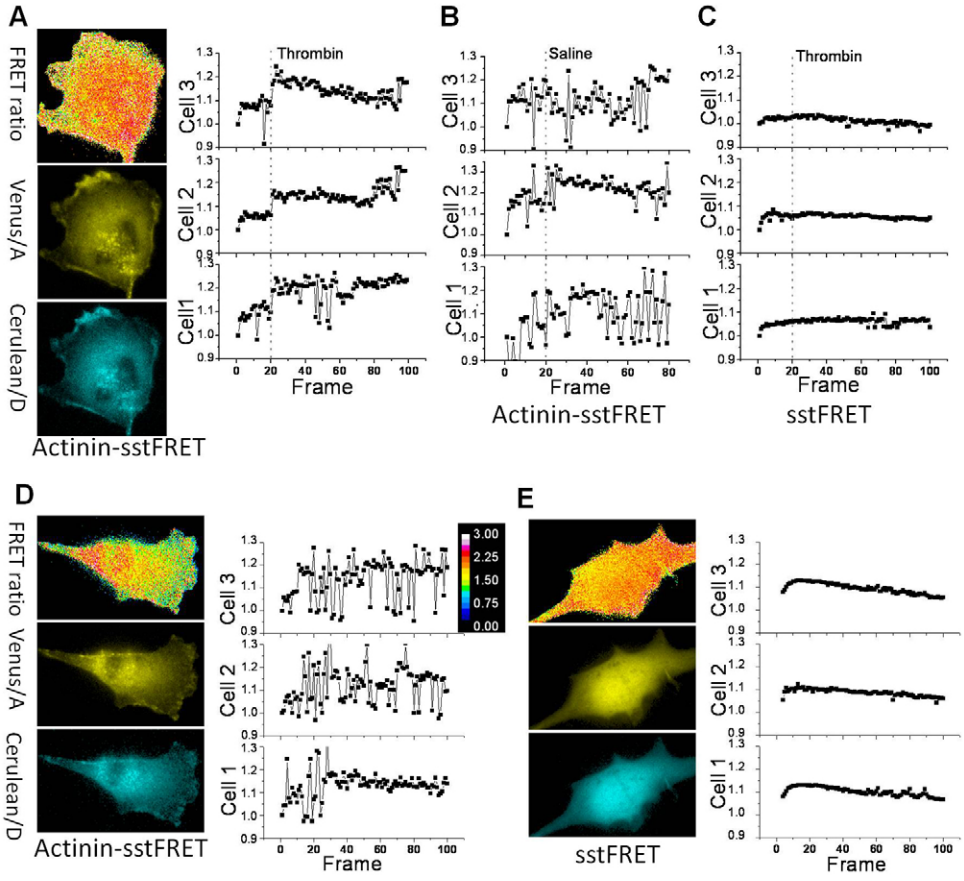

Fig. 6. Thrombin decreased cytoskeleton stress and reduced tension fluctuations in BAECs. (**A**) BAECs expressing actinin-sstFRET were recorded at 20-second intervals for 100 frames. Thrombin (5 units/ml) perfusion was started at the 20th time frame as marked by the vertical dotted line. Donor, acceptor and FRET ratios of the first frame for one cell are shown in the images on the left, and the FRET ratios of three individual cells are plotted on the right. (**B**) Control perfusion using plain saline produced no effect. The FRET ratios of three individual cells are plotted, and the vertical dotted line marks the 20th time frame after the initiation of perfusion. (**C**) Control BAECs expressing free sstFRET and treated with thrombin showed no change, illustrating that the thrombin effect was transmitted through actinin. (**D**) Actinin-sstFRET displayed a wider stress fluctuation and migrating cells show the stress heterogeneity in the leading and lagging edges. Actinin-sstFRET BAECs monitored at 3-second intervals for 100 frames. The first frame of FRET ratio, Venus/acceptor and Cerulean/donor channels are given on the left, and the FRET ratios of three individual cells are plotted on the right. The inset is the calibration bar of a 16 color lookup table. (**E**) Control, cells expressing free sstFRET displayed no FRET fluctuations, indicating that expression of sstFRET with actinin is necessary for observation of the physiological effects.

result of extreme osmotic pressure unfolding the spectrin linker and stretching it sufficiently so that there was no significant energy transfer. These osmotic effects on FRET were largely reversible, with FRET returning to 1.5 in normal saline (Fig. 7C). Thus, there was no lasting dissociation of actinin from the network or breakdown of the network itself.

Were these FRET changes due to mechanical stress in actinin or possibly the result of another environmental change? We applied similar challenges to cells coexpressing the unlinked donor and acceptor (Fig. 7D,F) and to cells expressing the free cassette (Fig. 7E,F). These cells showed similar morphological changes but no significant changes in FRET; the FRET changes were clearly coupled through actinin. This unstressed probe data again supports the FRET calculation method because large changes in cell volume (probe concentration) did not change FRET.

We saw similar results in BAECs (Fig. 8), but because BAECs could withstand 100% distilled water, we simply followed their behavior over time. We again detected the transient increase in FRET (decrease in tension). After 1 hour in distilled water, the cells were quite swollen and the actinin stress increased by more than 20% (FRET ratio changing from 1.8 to 1.4; Fig. 8A,B). Returning cells to bath saline caused them to shrink and to release the force on actinin (the FRET ratio increased by 14%, from 1.4 to 1.6; Fig. 8B,C). A second round of exposure to 100% distilled water swelled the cells even more dramatically, showing that the original stresses produced some long term remodeling. Following this second round of distilled water stimulation, the cells began detaching from the substrate and were fully rounded up within 3 hours. During this time, the actinin stress increased (FRET ratio from 1.6 to 1.3) and, as observed with the HEK cells, there was a plastic deformation of the cytoskeleton. The ability of BAECs to withstand an extreme osmotic challenge shows that they have a more robust cytoskeleton than HEK (under maximal stress the FRET in BAECs was 1.3 whereas that of HEKs was 1.1). The mechanical differences were mirrored by the differences in actinin distribution between the two cell types (cf. Fig. 2), but the basic integrity of the cytoskeleton in both cell types was preserved because we could see labeled fibers, even after the cells had been in distilled water for an hour (Fig. 8D).

The response of cells to a hypertonic challenge is more complex than that of a hypotonic challenge as a result of fiber buckling and excluded volumes. However, for the sake of generality, we challenged both HEKs and BAECs with hypertonic stress (supplementary material Fig. S5). We again observed the paradoxical transient response, but in this case it was a transient increase in tension. After 2 minutes, the cells shrank and the tension decreased. Returning the cells to normal saline caused the tension to increase again as actinin was stressed by swelling (supplementary material Fig. S5).

Discussion

An ideal mechanical sensor has to satisfy four requirements: genetic coding, force sensitivity, compliance that matches the host protein, and no interference with normal function of the host. With a FRET pair that is linearly elastic, the maximum sensitivity occurs when the nominal spacing is the characteristic Förster distance (Fanjie Meng; stFRET, a novel tool to study molecular force in living cells and animals, PhD thesis, State University of

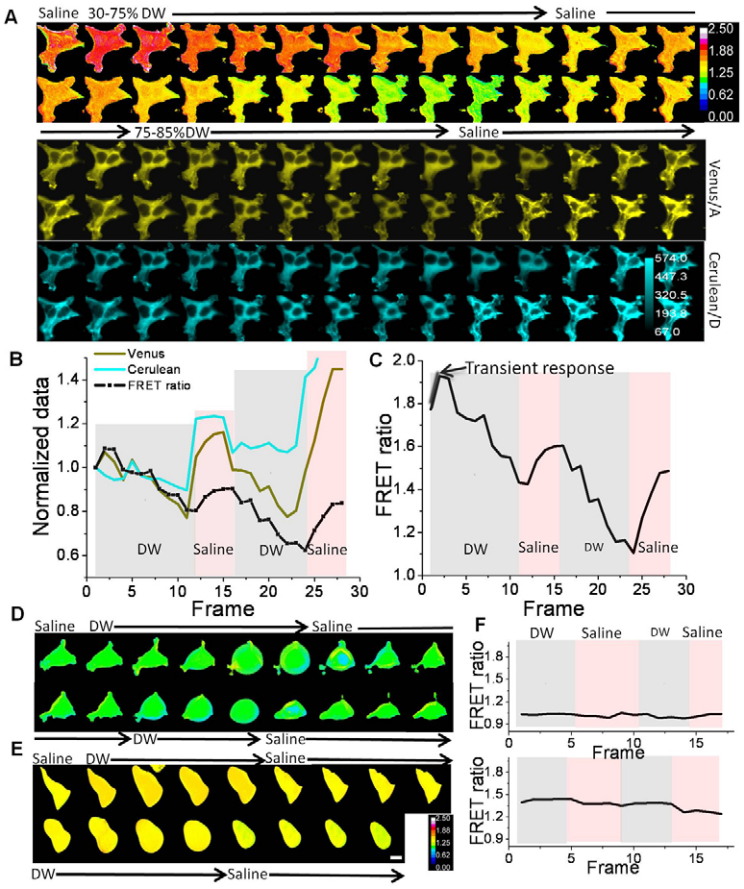

Fig. 7. Hypotonic challenge to HEKs stresses actinin. (**A**) Time-lapse images of the FRET ratio (upper panel), Venus/acceptor (middle panel) and Cerulean/donor (lower panel) images of actinin-sstFRET cells under different hypotonic challenges. The treatments were 30% distilled water (DW) for 20 minutes, then 50% DW for 20 minutes and 75% DW for 10 minutes; then the bath was exchanged to saline for 30 minutes; and then 75% DW for 20 minutes, 85% DW for 10 minutes; then saline for 30 minutes. FRET ratio images are displayed with a 16 color lookup table with a calibration bar from 0 to 2.5. Venus and Cerulean image intensities were assigned the colors yellow and cyan. (**B**) Mean values of Venus/acceptor, Cerulean/donor and FRET ratios for each frame of a single cell. Data were normalized to the first frame. (**C**) FRET ratio of actinin-sstFRET shows an opposite polarity transient response and an immediate increase of FRET during the first 2 minutes. Gray shadowing indicates distilled water and red shadowing indicates saline. (**D**,**E**) Data taken from a time-lapse series of FRET ratio images of a cell coexpressing Venus and Cerulean (D) and expressing plain sstFRET (E). The latter show no swelling, indicating that the observed changes in FRET with actinin-sstFRET arose through coupling to actinin. Cells were given a distilled water challenge then perfused with normal saline, and this cycle was repeated twice. Images are displayed as in A. (**F**) Average FRET ratio plot of each frame of a cell coexpressing Venus and Cerulean (upper panel) and plain sstFRET (lower panel) showing the flat FRET ratio through the time series. The hypoosmotic challenge cycles are marked as in B. Scale bar: 10 µm.

New York at Buffalo, 2008); Meng et al., 2008). A simple calculation shows that, at that operating point, FRET is linear with strain. If the linker were made more compliant in an effort to increase the force sensitivity, the probe would undergo larger thermal fluctuations that would tend to mask the improvement. However, if the force–distance relationship were nonlinear, because of domain unfolding (Ortiz et al., 2005), the relationship of FRET efficiency to strain could be improved, with a sacrifice in linearity. However, the issue of linearity is not crucial for experiments with optical imaging because these do not measure the response of single molecules, but the averages taken over the optical voxel. The voxel volume contains many molecules whose stress fluctuates in time and hence is also averaged over the duration of the exposure. The voxels are likely to contain regions with different stress as well as unlabeled components resulting from endogenous gene expression. Our experiments have focused on macroscopic gradients of stress (micrometer scale) and not on molecular stress. The genetic encoding allows us to specify that we are recording averages from a specific chemical species, but the finite resolution of optical imaging will not allow us to measure the stress in a given molecule.

The force sensitivity of sstFRET in solution measured with DNA springs showed that FRET is well modulated by forces in the range of 5–7 pN, forces clearly relevant to physiological levels of stress (cf. Fig. 1). The compliance of sstFRET will be comparable to that expected for α-actinin that has four of these repeats. The fluorophores themselves are stiff and will not be significantly deformed by biological stresses (Dietz and Rief, 2004). The correlation of intracellular stress to external physiological stress was made clear by Johnson and colleagues (Johnson et al., 2007), who showed that fluid shear stress applied to living cells can unfold spectrin repeats exposing cryptic cysteine residues within them.

We have shown that sstFRET can be incorporated into proteins with no changes in distribution relative to the more common terminal EGFP label (Figs 2–4). This result agrees with our earlier data on the probe stFRET that contains a helical linker (Fanjie Meng; stFRET, a novel tool to study molecular force in living cells and animals, PhD thesis, State University of New York at Buffalo, 2008); Meng et al., 2008). We have since created transgenic *Caenorhabditis elegans* with the probe inserted into collagen 19. When properly located in the sequence, the collagen distribution is normal and the worms behave normally (Meng et al., 2011, in press). Clearly the stress sensors can be made innocuous and can be used to assess protein stresses in cells, tissues, organs and animals.

The distinct distribution patterns of labeled actinin between HEKs and BAECs shows that gene expression and protein localization were fixed at an embryonic stage and remained remarkably stable for many passages in culture. What is the physiological utility of these different distributions? As kidney cells, HEKs might have evolved to be sensitive to osmotic stress, whereas BAECs evolved to withstand constitutive shear and wall stress. BAECs could withstand distilled water for hours (a transmembrane pressure >5 Atm) (Spagnoli et al., 2008; Wan et al., 1995) with a minimal shape change (Figs 7, 8). Thus, there are strong attachments between the upper and lower cell membranes, and these same links will make them resistant to shear stress.

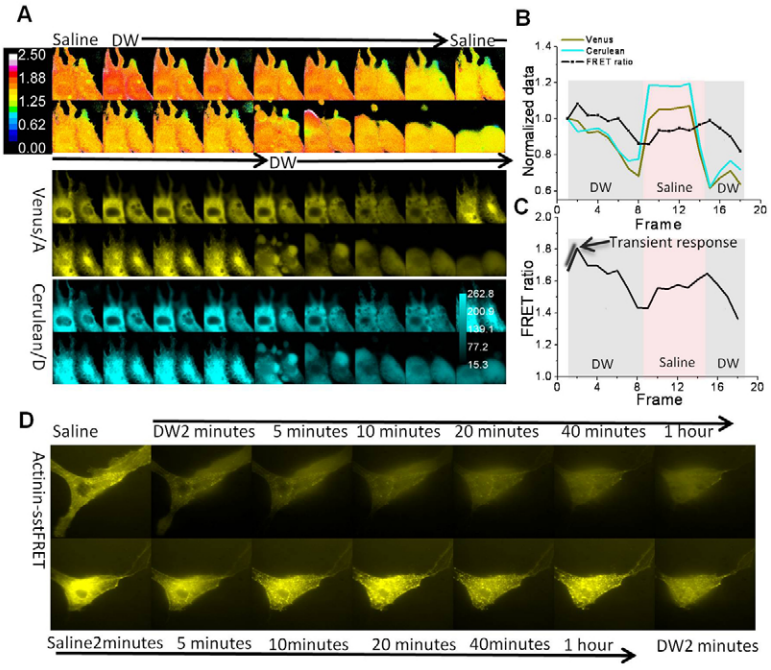

Fig. 8. Hypotonic stress increases the force on actinin-sstFRET in BAECs. (**A**) Time-lapse images of the FRET ratio (upper panel), Venus/acceptor (middle panel) and Cerulean/donor (lower panel) in cells challenged with distilled water (DW; 16 color lookup table with a calibration bar of 0 to 2.5; Venus and Cerulean assigned to yellow and cyan). (**B**) Average value of Venus/acceptor, Cerulean/donor and FRET ratio of the cell in each frame. (**C**) FRET ratio of actinin-sstFRET in BAECs under hypoosmotic challenge showing the opposite polarity transient during the first 2 minutes after hypotonic shock. Data are normalized and presented as described in Fig. 4. (**D**) Actinin-sstFRET BAEC cell under distilled water shock. Periodicity in the stress fibers remains visible even after 1 hour of exposure to distilled water and 1 hour saline recovery so that the actin/actinin structure is not destroyed by this extreme stimulus.

Stresses in actinin in resting cells were often not correlated with obvious changes in cell shape. When cells underwent contraction or expansion during random probing for migration (as in Fig. 5 and supplementary material Movies 1 and 2), sstFRET did not register a change in stress. Only after the cells started to migrate (see Fig. 5A,B, frame 23 and supplementary material Movies 1 and 2) did we observe significant changes. The minimal stress observed during random probing might partly reflect averaging over regions with nonuniform stress, i.e. FRET increases in one region and decreases in another. The paradoxical transient responses we observed with osmotic stress suggest that, at rest, the actinin axis is not parallel to the actin axis, and that increasing stress pulls on it and aligns it in a more parallel orientation allowing it to share more tension. Nearly all materials have a positive Poisson constant – objects get thinner when stretched – so that stretching actin can also cause orthogonally oriented actinin to be compressed. In BAECs, we observed large dynamic fluctuations of stress with lifetimes of seconds (Fig. 6). These fluctuations represent the active dynamics of the cytoskeleton and are not the result of photon noise because they are not seen with stress-free sstFRET (a detailed analysis of the actinin dynamics is in progress).

The results with osmotic challenge support the hypothesis that a significant component of osmotic stress is spread in three dimensions within the cytoskeleton and is not confined to the membrane (Spagnoli et al., 2008). Thus, the cell behaves not like a bag but like a sponge enclosed in a semipermeable membrane. The stress probes are clearly opening new areas of cell biology. We have begun to utilize the probes to explore stress in organs and whole animals by making transgenic mice containing labeled actinin driven by a universal actin promoter. These mice not only provide prelabeled cells of all tissues, but permit organ level analysis of stresses in real time. The mice develop and reproduce normally, emphasizing the innocuous nature of the actinin labeling (F.M. and F.S, unpublished results). We are now building a transgenic library with many different labeled cytoskeletal and extracellular proteins.

Conclusions

The compliance-matched sstFRET sensor is reliable, displays high sensitivity, and causes no interference with host protein function. The probe has revealed time-dependent spatial gradients of stress that promise to provide insights into a wide range of cell biology.

Materials and Methods

Protein–DNA complex synthesis and in vitro DNA stretching

A 60mer DNA, [AminoC6] GAGTGTGGAGCCTAGACCGTGAATTCCTGGCAG-TGGTGCGACCGACGTGGAGCCTCCCTC [AmC7Q], and the complementary strand were purchased from Operon (Huntsville, AL). The oligo has an amino modification on both ends and an *Eco*RI cutting site in the middle. The sequence was selected on the basis of a previously published study (Wan et al., 1995). 15 nmol of amino-tagged DNA were incubated with 300 nmol heterobifunctional crosslinker SMPB (succinimidyl 4-[*p*-maleimidophenyl] butyrate) (Pierce, Rockford, IL) in 20 µl conjugation buffer (100 mM sodium phosphate, 150 mM NaCl and 1 mM EDTA at pH 7.5) for 2 hours at room temperature. The amino groups of the DNA react with the NHS-ester group of the crosslinker. The reaction mixture was passed twice through protein desalting spin columns (Pierce, Rockford, IL) to remove excess uncoupled crosslinkers. The DNA–crosslinker construct was then incubated with 1.5 nmol of purified sstFRET protein in conjugation buffer with total volume 50 µl. Both donor and acceptor in sstFRET have two free sulfhydryl groups at cysteines 48 and 70. The 70 position is concealed inside the β-barrel and inaccessible, and the 48 position is only partially exposed to solution. In order to speed the reaction of the maleimides of the DNA–crosslinker complex to sulfhydryls at position 48, we incubated the mixture at 37°C for 30 minutes. Because DNA doesn't interfere with the FRET measurements, no further purification was necessary. To stretch sstFRET, 15 nmol of complementary DNA was added to protein–single strand DNA complex. The solution was left at room temperature overnight to complete the annealing.

Cell imaging and FRET ratio calculation

Cell imaging was performed on an inverted Zeiss Axio Observer A1 equipped with an Andor Ixon DV897 back-illuminated cooled CCD camera. The images at the donor emission wavelengths were recorded side by side using a Dual View (Photometrics) splitter with excitation alternately applied to the donor and acceptor with appropriate excitation filters.

We calculated the FRET ratio R using the relationship:

$$R = I_a / I_d \ , \qquad (1)$$

where I_a is the acceptor emission intensity with acceptor excitation and I_d is the donor emission intensity with donor excitation. The acceptor intensity scales with protein concentration and the donor signal scales with both protein concentration and quenching due to FRET. To calculate R without energy transfer, we used a dilute 1:1 mixture of the two fluorophores and obtained R=R_0=1.05 both in solution

(supplementary material Fig. S4) and in cells (Fig. 2). The FRET ratio of sstFRET in both cells (Fig. 2) and solution (supplementary material Fig. S4) was $R=R_{FRET}=1.42$.

The FRET efficiency E is defined as the relative change of intensity referenced to the same pair with no energy transfer:

$$E = (I_{\overline{aFRET}} - I_{dFRET}) / I_{\overline{aFRET}} , \quad (2)$$

where the subscript $_{dFRET}$ denotes the donor signal with energy transfer and $_{\overline{dFRET}}$ denotes the donor signal with no energy transfer. Combining equations (1) and (2):

$$E = \frac{I_{\overline{aFRET}}/R_{\overline{FRET}} - I_{aFRET}/R_{FRET}}{I_{\overline{aFRET}}/R_{\overline{FRET}}} , \quad (3)$$

In equation (3), $I_{\overline{aFRET}}$ is the acceptor signal with no energy transfer, and I_{aFRET} is acceptor signal with energy transfer. Because the acceptor signal only depends upon a concentration that is fixed at a given point in time, $I_{\overline{aFRET}}=I_{aFRET}$ and $R_{\overline{FRET}}$ is the ratio of the intensities without energy transfer, so that $R_{\overline{FRET}}=R_0$ is obtained from the 1:1 mixture of fluorophores.

Simplifying equation (3):

$$E = 1 - R_0/R_{FRET} , \quad (4)$$

which yields an efficiency for unstressed sstFRET of 26%.

For time series image acquisition, we used Metamorph software and a Lumencor LED illuminator from BioVision (Mountain View, CA). The 433 nm and 515 nm excitation power was set at 25% with an exposure time of 50 milliseconds for each time point, at 20 minutes intervals, over a total experimental time span of 1000 minutes.

Gene construction and protein purification

pEYFP–C1 Venus and pECFP–C1 Cerulean plasmids were generous gifts from David W. Piston. sstFRET gene construction was as described in our previous publication (Meng et al., 2008). The spectrin repeat linker was subcloned from non-erythrocytic 1 (α-fodrin) isoform 1 by primers 5′-GTACAGAGGAGATCTGGAGGCTTCCACA-GAGATGCTGATG-3′ and 5′-GTCACCCAAGAATTCACGCCTCCCTTTGC-CTTGCGCTG-3′. Then, sstFRET gene was subcloned into prokaryotic expression vector pET-52b (+) (Novagen, Gibbstown, NJ) for protein purification. *Bam*HI and *Not*I restriction sites were introduced into sstFRET DNA fragment by primers 5′-GCTTCAGCTGGGATCCGGTGGTATGGTGAGCAAGG-3′ and 5′-CCAGAT-CGCGGCCGCTTAGTGGTGATGATGGTGGTGATGATGCTTGTACAGCTCGTC C-3′. An 8-histidine tag followed by TAA stop codon was inserted in front of the *Not*I site to make sure that the tag was located in the C-terminal and well-exposed to solution.

To create chimeric gene constructs of α-actinin, we subcloned the actinin gene into pEYFP–C1 vector, where the YFP gene was removed beforehand. The primers and restriction enzyme sites introduced into PCR products for subcloning were: Actinin, sense, 5′-CAGATCCGCTAGCATGGACCATTATGATTCTCAGCAAA-CC-3′ with *Nhe*I, anti-sense, 5′-GATCCCGGGCCCGCGGTACCTTAGAGGT-CACTCTCGCCGTAC-3′ with *Kpn*I. sstFRET were inserted into actinin at position 300, which was located in the linker domain between first and second spectrin repeat domains by restriction sites *Age*I and *Not*I. The restriction enzyme sites were introduced into the host proteins using the site-directed mutagenesis kit from Stratagene (La Jolla, CA) with the host protein amino acid unchanged. All construct sequences were confirmed by DNA sequencing at Roswell-Park Cancer Institute (Buffalo, NY).

FRET ratio calculation and cell imaging

We used a fluorescence spectrometer (Aminco·Bowman series 2 luminescence spectrometer) to measure the fluorescence of purified proteins in solution. All purified proteins were exchanged into 10 mM Tris-HCl buffer before further processing. The measurement was performed at room temperature with 200 µl of 1 µM protein. The spectrometer was set to: 4 nm bandpass, 1 nm step size, and 450–600 nm emission scan range with excitation at 433 nm. We used the FRET ratio R as measure of the energy transfer index: $R=I_{\text{AsstFRET 527nm}}/I_{\text{DsstFRET475nm}}$ in which I_{AsstFRET} is the acceptor emission signal of sstFRET with excitation of the acceptor and I_{DsstFRET} is the donor emission signal with excitation of the donor.

Cells were observed at room temperature using an Axio Observer A1 inverted microscope (Carl Zeiss, Thornwood, NY) and images were captured by an Ixon, cooled and back-illuminated, CCD camera (Andor, Belfast, UK). Donor and acceptor signals were obtained using the donor filter set ET430/24X, ET470/24M and acceptor filter set ET500/20X, ET535/30M (Chroma, Rockingham, VT). Images were processed with ImageJ (http://rsb.info.nih.gov/ij). FRET ratio images were made using the equation $R=I_{\text{Venus acceptor}}/I_{\text{Cerulean donor}}$. Because the donor and acceptor channel were obtained independently with the specified filter sets, we needed no bleed-through correction. The donor and acceptor images were background subtracted before calculating the FRET ratio.

Cell culture, transfection and protein expressing

BAEC and HEK cells were cultured in Dulbecco's modified Eagle's medium (GIBCO Invitrogen, Carlsbad, CA) supplemented with 10% fetal bovine serum and antibiotics. Cells were spread on 3.5-mm coverslips and allowed to grow for 24 hours. Fugene 6 (Roche, Indianapolis, IN) was used to deliver 2.0 µg per coverslip of plasmid DNA to the cells. The cells were studied 24–36 hours following transfection.

We thank David Piston (Vanderbilt University) for providing us with the mVenus and mCerulean vectors, Thomas Suchyna for thoughtful discussion, Phil Gottlieb for advice on the chemistry, Mary Teeling for cell culture and Ed Hurley from BioVision for helping with Metamorph software and LED illuminator. Special thanks to Wade J. Sigurdson and the confocal microscope facility in the School of Medicine and Biomedical Sciences, University at Buffalo. This work was supported by a grant from US National Institutes of Health. Deposited in PMC for release after 12 months.

Supplementary material available online at
http://jcs.biologists.org/cgi/content/full/124/2/261/DC1

References

An, X., Zhang, X., Salomao, M., Guo, X., Yang, Y., Wu, Y., Gratzer, W., Baines, A. J. and Mohandas, N. (2006). Thermal stabilities of brain spectrin and the constituent repeats of subunits. *Biochemistry* **45**, 13670-13676.

Bogatcheva, N. V., Garcia, J. G. and Verin, A. D. (2002). Molecular mechanisms of thrombin-induced endothelial cell permeability. *Biochemistry* **67**, 75-84.

Bustamante, C., Chemla, Y. R., Forde, N. R. and Izhaky, D. (2004). Mechanical processes in biochemistry. *Annu. Rev. Biochem.* **73**, 705-748.

Coll, J. L., Ben-Ze'ev, A., Ezzell, R. M., Rodriguez Fernandez, J. L., Baribault, H., Oshima, R. G. and Adamson, E. D. (1995). Targeted disruption of vinculin genes in F9 and embryonic stem cells changes cell morphology, adhesion, and locomotion. *Proc. Natl. Acad. Sci. USA* **92**, 9161-9165.

Dietz, H. and Rief, M. (2004). Exploring the energy landscape of GFP by single-molecule mechanical experiments. *Proc. Natl. Acad. Sci. USA* **101**, 16192-16197.

du Roure, O., Saez, A., Buguin, A., Austin, R. H., Chavrier, P., Silberzan, P. and Ladoux, B. (2005). Force mapping in epithelial cell migration. *Proc. Natl. Acad. Sci. USA* **102**, 2390-2395.

Essler, M., Amano, M., Kruse, H. J., Kaibuchi, K., Weber, P. C. and Aepfelbacher, M. (1998). Thrombin inactivates myosin light chain phosphatase via Rho and its target Rho kinase in human endothelial cells. *J. Biol. Chem.* **273**, 21867-21874.

Garcia, J. G. (1992). Molecular mechanisms of thrombin-induced human and bovine endothelial cell activation. *J. Lab. Clin. Med.* **120**, 513-519.

Golji, J., Collins, R. and Mofrad, M. R. (2009). Molecular mechanics of the alpha-actinin rod domain: bending, torsional, and extensional behavior. *PLoS Comput. Biol.* **5**, e1000389.

Hwang, S. M., Li, J., Koo, N. Y., Choi, S. Y., Lee, S. J., Oh, S. B., Castro, R., Kim, J. S. and Park, K. (2009). Role of purinergic receptor in alpha fodrin degradation in Par C5 cells. *J. Dent. Res.* **88**, 927-932.

Iwai, S. and Uyeda, T. Q. (2008). Visualizing myosin-actin interaction with a genetically-encoded fluorescent strain sensor. *Proc. Natl. Acad. Sci. USA* **105**, 16882-16887.

Johnson, C. P., Tanbg, H. Y., Carag, C., Speicher, D. and Discher, D. E. (2007). Forced unfolding of proteins within cells. *Science* **317**, 663-666.

Kumar, S. and Weaver, V. M. (2009). Mechanics, malignancy, and metastasis: the force journey of a tumor cell. *Cancer Metastasis Rev.* **28**, 113-127.

Kung, C. (2005). A possible unifying principle for mechanosensation. *Nature* **436**, 647-654.

Law, R., Liao, G., Harper, S., Yang, G., Speicher, D. W. and Discher, D. E. (2003). Pathway shifts and thermal softening in temperature-coupled forced unfolding of spectrin domains. *Biophys. J.* **85**, 3286-3293.

Meng, F., Suchyna, T. M. and Sachs, F. (2008). A fluorescence energy transfer-based mechanical stress sensor for specific proteins in situ. *FEBS J.* **275**, 3072-3087.

Meng, F., Suchyna, T. M., Lazakovitch, E., Gronostajski, R. M. and Sachs, F. (2011). Real Time FRET Based Detection of Mechanical Stress in Cytoskeletal and Extracellular Matrix Proteins, *Cell. Mol. Bioeng.*, DOI: 10.1007. (*in press*).

Na, S., Collin, O., Chowdhury, F., Tay, B., Ouyang, M. X., Wang, Y. X. and Wang, N. (2008). Rapid signal transduction in living cells is a unique feature of mechanotransduction. *Proc. Natl. Acad. Sci. USA* **105**, 6626-6631.

Ortiz, V., Nielsen, S. O., Klein, M. L. and Discher, D. E. (2005). Unfolding a linker between helical repeats. *J. Mol. Biol.* **349**, 638-647.

Qu, H., Tseng, C. Y., Wang, Y., Levine, A. J. and Zocchi, G. (2010). The elastic energy of sharply bent nicked DNA. *Europhys. Lett.* **90**, 18003

Shyu, K. G. (2009). Cellular and molecular effects of mechanical stretch on vascular cells and cardiac myocytes. *Clin. Sci.* **116**, 377-389.

Sjoblom, B., Salmazo, A. and Djinovic-Carugo, K. (2008). Alpha-actinin structure and regulation. *Cell. Mol. Life Sci.* **65**, 2688-2701.

Spagnoli, C., Beyder, A., Besch, S. and Sachs, F. (2008). Atomic force microscopy analysis of cell volume regulation. *Phys. Rev. E. Stat. Nonlin. Soft Matter Phys.* **78**, 031916.

Tseng, C. Y., Wang, A., Zocchi, G., Rolih, B. and Levine, A. J. (2009). Elastic energy of protein-DNA chimeras. *Phys. Rev. E. Stat. Nonlin. Soft Matter Phys.* **80**, 061912.

Vogel, V. and Sheetz, M. (2006). Local force and geometry sensing regulate cell functions. *Nat. Rev. Mol. Cell Biol.* **7**, 265-275.

Wallace, G. Q. and McNally, E. M. (2009). Mechanisms of muscle degeneration, regeneration, and repair in the muscular dystrophies. *Annu. Rev. Physiol.* **71**, 37-57.

Wan, X., Harris, J. A. and Morris, C. E. (1995). Responses of neurons to extreme osmomechanical stress. *J. Membr. Biol.* **145**, 21-31.

Zocchi, G. (2009). Controlling proteins through molecular springs. *Annu. Rev. Biophys.* **38**, 75-88.